Chiral quark model with infrared cut-off for the description of meson properties in hot matter

D. Blaschke, G. Burau

Fachbereich Physik, Universität Rostock,
D-18051 Rostock, Germany

M. K. Volkov, and V. L. Yudichev

Bogoliubov Laboratory of Theoretical Physics,
Joint Institute for Nuclear Research,
141980 Dubna, Russian Federation

July 12, 2001

Abstract

A simple chiral quark model of the Nambu–Jona-Lasinio (NJL) type with a quark confinement mechanism is constructed for the description of the light meson sector of QCD at finite temperature. Unphysical quark production thresholds in the NJL model are excluded by an infrared cut-off in the momentum integration within quark loop diagrams. This chiral quark model satisfies the low energy theorems. Using the vacuum masses and decay widths of π- and ρ-mesons for fixing the model parameters, the properties of the σ- meson are derived. Within the Matsubara formalism, the model is systematically extended to finite temperatures where chiral symmetry restoration due to a dropping constituent quark mass entails a vanishing of the infrared cut-off (deconfinement) at the pion Mott temperature $T_c = 186$ MeV. Besides of the pion mass and weak decay constant, the masses, coupling constants and decay widths of σ- and ρ-mesons in hot matter are investigated. The quark-antiquark decay channel of the light mesons is opened for $T > T_c$ only and becomes particularly strong for the ρ- meson. The two-pion decay channel below T_c has almost constant width for the ρ- meson up to T_c, but for the σ-meson it closes below T_c such that a scalar meson state with vanishing width is obtained as a precursor of the chiral/deconfinement transition.

PACS numbers: 11.30.Rd, 12.38.Lg, 13.25.-k, 11.10.Wx

1 Introduction

One of the most interesting phenomena predicted by QCD for a hot and dense matter is the existence of the quark-gluon plasma (QGP) phase [1], where hadrons do not exist as bound states, and the strongly interacting matter should be described in terms of QCD fundamental fields: quarks and gluons. A number of modern experiments have been already directed on the search of signals that can be interpreted as evidence for the existence of the QGP, and still new projects are upcoming. The most straightforward experiment, where QGP is hoped to be found is a collision of heavy ions with ultra-relativistic energies, where hadrons form so hot and dense matter that the conditions necessary for QGP creation are fulfilled. However, one cannot tell certainly if QGP was seen or not without laying a proper theoretical ground for such an experiment. Actually, one needs to know what is to be expected in order to unambiguously detect the QGP is formed. Taking into account that a direct modelling of QGP from QCD is not available at present, one needs an appropriate quark model which would reflect the most important features of strong interactions, on the one hand, and would be tractable, on the other hand. Among the various approaches, one can select the Nambu–Jona-Lasinio (NJL) model.

The Nambu–Jona-Lasinio model is a convenient semiphenomenological quark model for the description of the low energy meson physics [2, 3, 4, 5, 6]. Within this model the mechanism of spontaneous breaking of chiral symmetry (SBCS) is realized in a simple and transparent way, and the low energy theorems are fulfilled.

However, the ordinary NJL model fails to prevent hadrons from decaying into free quarks, which makes the realistic description of hadron properties on their mass shell questionable. The solution of this problem seems to be a very difficult task, and different methods have been proposed for this purpose [7, 8, 9, 10, 11, 12]. In our previous papers [13, 14, 15], a chiral quark model was suggested where unphysical quark-antiquark thresholds were eliminated by means of an infrared (IR) cut-off. As a result, the pole of the integrand in a quark loop integral turned out to be outside the integration interval, so that no imaginary part occurs.

This method of modeling the phenomenon of confinement is based on the idea of combining the NJL [2, 3, 4, 5, 6] and bag models [16, 17, 18]. Together with the ultraviolet (UV) cut-off, which is necessary to eliminate the UV divergence, we introduce the IR cut-off and thereby divide the momentum space into three domains. In Fig. 1 these domains are represented schematically in the coordinate space.

The first domain corresponds to short distances (large momenta), where quarks are not confined and the chiral symmetry is not spontaneously broken. This domain is excluded by the UV cut-off Λ.

In the second domain, SBCS takes place, and the quark condensate appears, which leads to the replacement of the current quarks by constituent ones. According to the idea of the bag-model, it is necessary to assume that quarks are not allowed to propagate over distances exceeding the dimensions of a bag. In the language of quark-loop integrals, this leads to a low momenta, infrared (IR), cut-off λ that provides the confinement of quarks.

In [13, 14, 15], the IR cut-off λ was chosen to be proportional to the constituent quark

mass m: $\lambda = c\,m$, where the arbitrary parameter c was the same for all mesons. At $c \sim 2$, the nonphysical quark-antiquark thresholds were absent for the π-, σ-, and ρ-mesons in the vacuum. However, in hot matter, these thresholds appeared at certain temperatures which, on the one hand, did not coincide with the chiral symmetry restoration (CSR) temperature T_c and, on the other, were different for various sorts of mesons.

In the present work, we suggest a new version of the model with an IR cut-off which differs from that given in [13, 14, 15] in two main points. First, we suggest that the IR cut-off is different for various mesons and increases with the mass of the corresponding meson. Second, the deconfinement phase transition occurs at a certain temperature $T_{\rm c}$, unique for all mesons, which coincides with the CSR temperature. In order to define this critical temperature uniquely also away from the chiral limit, we will identify it with the pion Mott temperature. Above this temperature the pion (and also the other mesons) are no longer bound states but resonances in the $q\bar{q}$ continuum instead.

We use our model to investigate the behavior of the constituent quark mass, the pion weak decay constant F_π, and the masses and coupling constants of the π-, σ- and ρ-mesons within the temperature interval up to the CSR and deconfinement phase transition. Very interesting effects at high temperature are revealed for the σ particle. The σ-meson, while having a noticeable width for the decay into two pions in the vacuum, can appear as a very narrow resonance in some processes occurring in hot and dense matter. This may lead to a significant enhancement of the dilepton and $\gamma\gamma$ production in the processes $\pi\pi \to e^+e^-$ and $\pi\pi \to \gamma\gamma$ near the phase transition [19, 20]. Detailed calculations of the effect of excess low-energy photon production in the process $\pi\pi \to \gamma\gamma$ have been performed in [20] (see also [21]). These effects can be understood as precursors of the phase transition between hadron matter and the QGP to be investigated in heavy-ion collisions performed e.g. at CERN SPS, at the new Brookhaven relativistic heavy ion collider (RHIC) [22] or at future facilities dedicated to the QGP search. Note that in [19, 20] a simple version of the NJL model was used, where the confinement of quarks had not been taken into account. Insofar as the confinement is important for the study of the phase transition of hadron matter to QGP, we then suggest here a new version of the model, with quark confinement.

Our paper is organized as follows. In Sect. 2, we give the effective chiral quark Lagrangian and the gap equation describing SBCS. Here, the pion mass formula in the IR cut-off scheme is obtained, and it is shown that the pion is a Goldstone boson in the chiral limit. In Sect. 3, the scalar meson (σ) is considered, and it is demonstrated that the quark loop with two σ-meson legs does not have an imaginary part when the IR cut-off λ is used. The model parameters are fitted in Sect. 4. In Sect. 5, the σ-meson mass and the $\sigma \to 2\pi$ decay width are estimated. In Sect. 6, we introduce a finite temperature generalization of the model and analyze results. In the last section, we discuss the obtained results and give a short outlook to further development of this model.

2 SU(2)×SU(2) Lagrangian, the gap equation and the pion mass formula

Let us consider an SU(2)×SU(2) NJL model defined by the Lagrangian

$$\begin{aligned}\mathcal{L}_q &= \bar{q}(i\partial\!\!\!/ - m^0)q + \frac{G_1}{2}\left[(\bar{q}q)^2 + (\bar{q}i\gamma_5\vec{\tau}q)^2\right] \\ &\quad -\frac{G_2}{2}\left[(\bar{q}\gamma_\mu\vec{\tau}q)^2 + (\bar{q}\gamma_5\gamma_\mu\vec{\tau}q)^2\right], \end{aligned} \tag{1}$$

where q and $\bar{q}$ are quark fields, and G_1 and G_2 are the constants that describe the interaction of quarks in the scalar (pseudoscalar) and vector (axial-vector) channels. The notation $\vec{\tau}$ is used for Pauli matrices, represented here as components of an isovector. This Lagrangian is chirally symmetric except for the term containing the current quark mass m^0.

As usual, one applies a bosonization procedure [3, 4] to the quark Lagrangian and obtains its equivalent representation in terms of the scalar (σ), pseudoscalar ($\vec{\pi}$), vector ($\vec{\rho}_\mu$) and axial-vector ($\vec{a}_{1\,\mu}$) meson fields

$$\begin{aligned}\mathcal{L}_{\rm mes} &= -\frac{\tilde{\sigma}^2 + \vec{\pi}^2}{2G_1} + \frac{\vec{\rho}_\mu^{\ 2} + \vec{a}_{1\,\mu}^2}{2G_2} \\ &\quad -i{\rm Tr}\ln\left\{1+\frac{1}{i\partial\!\!\!/ - m}[\sigma + i\gamma_5\vec{\tau}\vec{\pi} + \vec{\tau}\hat{\vec{\rho}} + \gamma_5\vec{\tau}\hat{\vec{a}}_1]\right\}. \end{aligned} \tag{2}$$

Here, the scalar fields σ and $\tilde{\sigma}$ are connected by the relation

$$-m^0 + \tilde{\sigma} \;=\; -m + \sigma\ . \tag{3}$$

The vacuum expectation value of $\tilde{\sigma}$ is non-zero after SBCS and new notation for the fluctuating part σ of the scalar field with zero vacuum expectation value, $\langle\sigma\rangle_0 = 0$, is introduced here. The vector $\hat{\vec{\rho}}$ and axial-vector $\hat{\vec{a}}_1$ fields are members of the Dirac algebra: $\hat{\vec{\rho}} = \vec{\rho}_\mu\gamma^\mu$, $\hat{\vec{a}}_1 = \vec{a}_{1\,\mu}\gamma^\mu$. Then, from the condition

$$\left.\frac{\delta\mathcal{L}_{\rm mes}}{\delta\sigma}\right|_{\sigma=0,\,\vec{\pi}=0} = 0\ \ , \tag{4}$$

one obtains the gap equation

$$m^0 = m[1 - 8G_1 I_1^\Lambda(m)] = m + 2G_1\langle\bar{q}q\rangle_0\ , \tag{5}$$

where $\langle\bar{q}q\rangle_0$ is the quark condensate. The quantity $I_1^\Lambda(m)$ is obtained from the quadratically divergent integral $I_1^\infty(m)$ by regularization with the UV cut-off Λ,

$$\begin{aligned} I_1^\Lambda(m) &= -i\frac{N_c}{(2\pi)^4}\int\frac{d^4k}{m^2 - k^2 - i\varepsilon}\theta(\Lambda^2 - |k_\perp|^2) \\ &= \frac{N_c}{(2\pi)^2}\int^\Lambda d{\rm k}\frac{{\rm k}^2}{E_{\rm k}} \\ &= \frac{N_c}{8\pi^2}\left[\Lambda\sqrt{\Lambda^2+m^2} - \ln\left(\frac{\Lambda + \sqrt{\Lambda^2+m^2}}{m}\right)\right], \end{aligned} \tag{6}$$

where $E_{\rm k} = \sqrt{{\rm k}^2 + m^2}$, $k_\perp$ is the 4-momentum of a quark, transverse to an arbitrary momentum P ($P^2 \neq 0$) (see [23, 24])

$$k_{\perp\mu} = k_\mu - P_\mu \frac{P\cdot k}{P^2}\ , \tag{7}$$

so that for $P = (M, 0, 0, 0)$ one has $k_\perp = (0, {\rm k}_1, {\rm k}_2, {\rm k}_3)$; N_c is the number of colors. For all applications of the model, we do not introduce an IR cut-off in $I_1^\Lambda(m)$.

Now let us consider the free part of Lagrangian (2) for pion fields in the quark one-loop approximation (see Fig. 2) [1]

$$\mathcal{L}_\pi^{(2)} = -\frac{\vec{\pi}^2}{2}\left\{\frac{1}{G_1} - 8I_1^\Lambda(m) - 4P^2 I_2^{(\lambda_P\,\Lambda)}(P,m)\right\}\ , \tag{8}$$

where $I_2^{(\lambda_P,\Lambda)}(P,m)$ is obtained from the logarithmically divergent integral $I_2^{(0,\infty)}(P,m)$ by applying IR- and UV- cut-offs

$$\begin{aligned} I_2^{(\lambda_P,\Lambda)}(P,m) &= \\ &= -i\frac{N_c}{(2\pi)^4}\int \frac{\theta(\Lambda^2 - |k_\perp|^2)\theta(|k_\perp|^2 - \lambda_P^2)d^4k}{(m^2 - k^2 - i\varepsilon)(m^2 - (k-P)^2 - i\varepsilon)} \\ &= \frac{N_c}{2\pi^2}\int_{\lambda_P}^{\Lambda} d{\rm k}\frac{{\rm k}^2}{E_{\rm k}(4E_{\rm k}^2 - P^2)}\ . \end{aligned} \tag{9}$$

Here, P is the momentum of a bound $\bar{q}q$ state (meson) and λ_P is an infrared cut-off introduced in order to remove unphysical quark-antiquark production thresholds, see Sect. 3. The last integration in (9) is done in the rest frame of a meson ($\mathbf{P} = 0$). The integral $I_2^{(\lambda_P,\Lambda)}(P,m)$ thereby depends on a Lorentz invariant, the meson mass M. Further, we prefer to consider $I_2^{(\lambda_P,\Lambda)}(P,m)$ as a function of M:

$$I_2^{(\lambda_M,\Lambda)}(M,m) \equiv I_2^{(\lambda_P,\Lambda)}(P,m)\Big|_{P=(M,0,0,0)}\ . \tag{10}$$

To express (8) through physical fields, we renormalize the pion

$$\vec{\pi} \ = \ g_\pi(M_\pi)\vec{\pi}^r, \tag{11}$$

$$g_\pi(M_\pi) \ = \ [4I_2^{(\lambda_{M_\pi},\Lambda)}(M_\pi,m)]^{-1/2}. \tag{12}$$

For the pion, there is also an additional renormalization factor $\sqrt{Z}$ appearing after we take into account $\pi - a_1$ transitions [4]:

$$\bar{g}_\pi = g_\pi\sqrt{Z}, \qquad Z^{-1} = 1 - \frac{6m^2}{M_{a_1}^2}, \tag{13}$$

where $M_{a_1} = 1230$ MeV is the mass of the a_1-meson. Thus, we obtain the following expression for the pion mass:

$$M_\pi^2 = \bar{g}_\pi^2(M_\pi)\left[\frac{1}{G_1} - 8I_1^\Lambda(m)\right]. \tag{14}$$

[1] The expression enclosed in parentheses can be written in the form $1/G_1 + \Pi_\pi(p)$, where $\Pi_\pi(p)$ is the pion polarization operator.

It can be given the form of the Gell-Mann–Oakes–Renner relation

$$M_\pi^2 \approx -2\frac{m^0\langle\bar{q}q\rangle_0}{F_\pi^2}, \tag{15}$$

where the Goldberger-Treiman relation (see (24) below) and the gap equation (5) have been used. One can see that this pion mass formula is in accordance with the Goldstone theorem since, for $m^0 = 0$, the pion mass vanishes and the pion becomes a Goldstone boson.

3 The σ-meson and IR confinement

The free part of Lagrangian (2) for the σ-meson in the one-loop approximation (see Fig. 2) has the following form

$$\mathcal{L}_\sigma^{(2)} = -\frac{\sigma^2}{2}\Big\{\frac{1}{G_1} - 8I_1^\Lambda(m) - 4(P^2 - 4m^2)I_2^{(\lambda_{M_\sigma},\Lambda)}(P,m)\Big\}. \tag{16}$$

After the renormalization of the σ field,

$$\sigma = g_\sigma(M_\sigma)\sigma^r, \tag{17}$$

$$g_\sigma(M_\sigma) = [4I_2^{(\lambda_{M_\sigma},\Lambda)}(M_\sigma,m)]^{-1/2}, \tag{18}$$

one obtains the expression for the σ-meson mass

$$M_\sigma^2 = g_\sigma^2(M_\sigma)\left[\frac{1}{G_1} - 8I_1^\Lambda(m)\right] + 4m^2. \tag{19}$$

Now, let us consider more carefully the integral

$$I_2^{(\lambda_{M_\sigma},\Lambda)}(M_\sigma,m) = \frac{N_c}{2\pi^2}\int_{\lambda_{M_\sigma}}^{\Lambda} d\mathrm{k}\frac{\mathrm{k}^2}{E_\mathrm{k}(4E_\mathrm{k}^2 - M_\sigma^2)}. \tag{20}$$

If $\lambda_{M_\sigma} = 0$, this integral has an imaginary part. Indeed, the integrand in (20) is singular when its denominator is equal to zero:

$$4E_\mathrm{k}^2 - M_\sigma^2 = 0. \tag{21}$$

The imaginary part appears when the singularity ($\mathrm{k} = \frac{1}{2}\sqrt{M_\sigma^2 - 4m^2}$) lies within the integration interval. Therefore, when one applies the IR cut-off

$$\lambda_P = [m_\mathrm{c}\,\theta(m - m_\mathrm{c}) + m\,\theta(m_\mathrm{c} - m)] \times\theta(P^2 - 4m_\mathrm{c}^2)\sqrt{\frac{P^2}{4m_\mathrm{c}^2} - 1}, \tag{22}$$

the denominator of integral (20) has no zero if the new model parameter m_c is smaller then the constituent quark mass. Thus, integral (20) is real, and the quark-antiquark production threshold is absent. We consider this property as a criterion for the quark confinement. It is different from that of the absence of real mass poles in the quark propagator, which is employed within the DSE approach [10, 11]. The parameter m_c is unique for all mesons and provides the $\bar{q}q$ thresholds after the temperature exceeds the critical value T_c. The temperature dependence of the meson properties following from this definition of the model will be investigated in detail in Sect. 6.

4 Model parameters

In the present model, there are five parameters: the constituent quark mass m, the 3D UV cut-off parameter Λ, the scalar (pseudoscalar) four-quark coupling constant G_1, the vector (axial-vector) four-quark coupling constant G_2, and the parameter $m_{\rm c}$. To fix our parameters, we use only four observables [25]: the pion weak decay constant $F_\pi = 93$ MeV, the $\rho \to \pi\pi$ decay constant $g_\rho^{\rm exp} = 6.14$, the pion mass $M_\pi = 140$ MeV, the ρ-meson mass $M_\rho = 770$ MeV, and the model parameter $m_{\rm c}$, determined as $m_{\rm c} = m(T_{\rm c})$. The value of $T_{\rm c}$ shall be the temperature above which the lightest meson can decay into free quarks (pion Mott temperature), which is defined by the formula:

$$2m(T_{\rm c}) = M_\pi(T_{\rm c}). \tag{23}$$

We find that $T_{\rm c} \approx 186$ MeV, and $m_{\rm c} \approx 86$ MeV, see Sect. 6. To fix m, Λ, G_1, and G_2, we use this value of $m_{\rm c}$ and the following four equations:

1) The Goldberger–Treiman relation

$$\frac{m}{F_\pi} = \bar{g}_\pi(M_\pi) = g_\pi(M_\pi)\sqrt{Z}. \tag{24}$$

2) The $\rho^0 \to \pi^+\pi^-$ decay width. The amplitude of this process is of the form

$$A_{\rho\to 2\pi} = i g_\rho^{\rm exp}(p_{\pi^+} - p_{\pi^-})^\nu \rho^0_\nu \pi^+\pi^-. \tag{25}$$

In the one-loop approximation, we obtain the following expression for $g_\rho^{\rm exp}$

$$g_\rho^{\rm exp} = 4Z^{-1} g_\rho(M_\rho)\bar{g}_\pi^2(M_\pi)\left[I_2^{(\lambda_{M_\rho},\Lambda)}(M_\rho, m) + 2M_\pi^2 J_{3V}^{\lambda_{M_\rho}}(M_\rho, M_\pi, m)\right], \tag{26}$$

where $g_\rho(M_\rho) = [\frac{2}{3} I_2^{(\lambda_{M_\rho},\Lambda)}(M_\rho, m)]^{-1/2}$ and the integral $J_{3V}^{\lambda_{M_\rho}}(M_\rho, M_\pi, m)$ is:

$$J_{3V}^{\lambda_{M_\rho}}(M_\rho, M_\pi, m) = \frac{1}{M_\rho^2 - 4M_\pi^2}\left(I_2^{(\lambda_{M_\rho},\Lambda)}(M_\rho, m) - \tilde{I}_2^{(\lambda_{M_\rho}\,\Lambda)}(M_\pi, m|M_\rho) - M_\pi^2 I_3^{\lambda_{M_\rho}}(M_\rho, M_\pi, m)\right), \tag{27}$$

where the integrals $I_2^{(\lambda_{M\rho},\Lambda)}(M_\pi, m|M_\rho)$ and $I_3^{\lambda_{M_\rho}}(M_\rho, M_\pi, m)$ are given below:

$$\tilde{I}_2^{(\lambda_{M_\rho},\Lambda)}(M_\pi, m|M_\rho) = \frac{N_c}{16\pi^2}\int\limits_{\lambda_{M_\rho}}^{\Lambda} \frac{{\rm k}d{\rm k}}{E_{\rm k}|\vec{p}\,|} \times \ln\left(\frac{(M_\pi^2 + 2{\rm k}|\vec{p}\,|)^2 - E_{\rm k}^2 M_\rho^2}{(M_\pi^2 - 2{\rm k}|\vec{p}\,|)^2 - E_{\rm k}^2 M_\rho^2}\right), \tag{28}$$

$$I_3^{\lambda_{M_\rho}}(M_\rho,M_\pi,m)=\frac{N_c}{16\pi^2}\int\limits_{\lambda_{M_\rho}}^{\infty}\frac{\mathrm{k}d\mathrm{k}}{|\vec{p}|E(M_\rho^2-4E^2)}$$
$$\times\left[\ln\left(\frac{(M_\pi^2+2\mathrm{k}|\vec{p}|)^2-E^2M_\rho^2}{(M_\pi^2-2\mathrm{k}|\vec{p}|)^2-E^2M_\rho^2}\right)\right.$$
$$\left.+\frac{M_\rho}{2E}\ln\left(\frac{M_\pi^4-(EM_\rho-2\mathrm{k}|\vec{p}|)^2}{M_\pi^4-(EM_\rho+2\mathrm{k}|\vec{p}|)^2}\right)\right]. \tag{29}$$

Here, $|\vec{p}|=\sqrt{M_\rho^2/4-M_\pi^2}$ is the 3-momentum of a pion after the decay of a ρ-meson in the rest frame of ρ.

The factor Z^{-1} appears due to $\pi-a_1$ transitions (see [4]). From these two equations one can find m and Λ.

3) The coupling constant G_1 is determined by the pion mass formula

$$M_\pi^2=\bar{g}_\pi^2(M_\pi)\left[\frac{1}{G_1}-8I_1^\Lambda(m)\right]. \tag{30}$$

4) The coupling constant G_2 is found from the mass formula for M_ρ [4]

$$M_\rho^2=\frac{g_\rho^2(M_\rho)}{4G_2}=\frac{3}{8G_2I_2^{(\lambda_{M_\rho},\Lambda)}(M_\rho,m)}. \tag{31}$$

From the gap equation (5), one gets the current quark mass m^0. The results of the parameter fixing procedure described above are summarized in Table 1. For the experimental values of the mass and width of the σ-meson, there is a wide uncertainy. The average limits for the mass are reported to be from 400 MeV to 1200 MeV (see [25, 26, 27]), and for the width: from 600 MeV to 1000 MeV. However, smaller values were also obtained: 290±54 MeV [28], 119±13 MeV [29].

5 The σ-meson mass and the decay $\sigma\to 2\pi$

The mass of the σ-meson is given by Eq. (19). Using this formula for $m_{\rm c}=86$ MeV (see Sect. 6) we obtain

$$M_\sigma=500\ \mathrm{MeV}. \tag{32}$$

The decay $\sigma\to 2\pi$ is described by the quark triangle diagram (see Fig. 3).

The amplitude of the process $\sigma\to 2\pi$ has the form

$$A_{\sigma\to 2\pi}=8mg_\sigma(M_\sigma)\bar{g}_\pi^2(M_\pi)[I_2^{(\lambda_{M_\sigma},\Lambda)}(M_\sigma,m)$$
$$+\mathcal{J}(M_\sigma,M_\pi,m)]\sigma\vec{\pi}^2\quad, \tag{33}$$

where

$$\mathcal{J}(M_\sigma,M_\pi,m)=-\frac{1}{2}(M_\sigma^2-2M_\pi^2)I_3^{\lambda_{M_\sigma}}(M_\sigma,M_\pi,m). \tag{34}$$

Then the decay width of the σ-meson is equal to

$$\begin{aligned}\Gamma_{\sigma\to 2\pi} &= \frac{3}{2\pi}\left(\frac{m^3(1+\delta)}{g_\sigma(M_\sigma)F_\pi^2 M_\sigma}\right)^2\sqrt{M_\sigma^2-4M_\pi^2}\\ &= 205\ \text{MeV}. \end{aligned} \tag{35}$$

where

$$\delta = \frac{\mathcal{J}(M_\sigma, M_\pi, m)}{I_2^{(\lambda_{M_\sigma},\Lambda)}(M_\sigma, m)} = -0.33\ . \tag{36}$$

Therefore, one can see that our estimates for the σ-meson mass are in agreement with experimental data [25] (see also [26, 27, 28, 29]) $M_\sigma^{\rm exp} = (400-1200)$ MeV. Let us note that the corrections coming from $\mathcal{J}$ are important for the calculation of the decay width. Indeed, a similar contribution to the $\rho\to\pi\pi$ decay width (see (27)) is small, whereas, in the case of the decay $\sigma\to\pi\pi$, it makes 30% of the amplitude and decreases the decay width by half. From this, one can conclude that the NJL model with the IR cut-off satisfies both of the low energy theorems together with SBCS and gives a satisfactory description of the low-energy physics of the scalar, pseudoscalar and vector mesons.

6 Finite temperature case

An interesting application of our model is the description of meson properties in a hot and dense medium. The standard NJL model has been already used for this purpose in [6, 30, 31], where the temperature dependence of quark and meson masses and of Yukawa coupling constants was found.

The calculation of the constituent quark and meson masses at finite temperature can be done in the imaginary time formalism [32, 33]. In all the quark loop diagrams, now we sum over Matsubara frequencies $\omega_n = (2n+1)\pi T$ instead of integrating over the energy component of the internal quark 4-momentum. As a result, for the integral $I_1^\Lambda(m)$ one has

$$\begin{aligned} &I_1^\Lambda(m,T) = \\ &\quad -i\frac{N_c}{(2\pi)^4}\int d^4k\frac{\theta(\Lambda^2-|k_\perp|^2)}{m(T)^2-k^2}\tanh\left(\frac{E_{k_\perp}}{2T}\right), \end{aligned} \tag{37}$$

$$E_{k_\perp} = \sqrt{|k_\perp|^2+m^2}\ . \tag{38}$$

The integral $I_2^{(\lambda_M,\Lambda)}(M,m,T)$ for a meson at rest $P=(M,0,0,0)$ in the rest frame of the heat bath is given by

$$\begin{aligned} &I_2^{(\lambda_M,\Lambda)}(M,m,T) = \\ &\quad -i\frac{N_c}{(2\pi)^4}\int d^4k\frac{\theta(\Lambda^2-|k_\perp|^2)\theta(|k_\perp|^2-\lambda_M^2)}{[m(T)^2-k^2][m(T)^2-(k+P)^2]} \\ &\quad \times\tanh\left(\frac{E_{k_\perp}}{2T}\right)\ . \end{aligned} \tag{39}$$

For the integrals $\tilde{I}_2$ and I_3, one obtains:

$$\tilde{I}_2^{(\lambda_{M_\rho},\Lambda)}(M_\pi,m,T|M_\rho)=\frac{N_c}{16\pi^2}\int\limits_{\lambda_{M_\rho}}^{\Lambda}d\mathrm{k}\frac{\mathrm{k}\tanh\left(\frac{E_\mathrm{k}}{2T}\right)}{E_\mathrm{k}|\vec{p}|}$$
$$\times\ln\left(\frac{(M_\pi^2-2\mathrm{k}|\vec{p}|)^2-E_\mathrm{k}^2M_\rho^2}{(M_\pi^2+2\mathrm{k}|\vec{p}|)^2-E_\mathrm{k}^2M_\rho^2}\right), \tag{40}$$

$$I_3^{\lambda_{M_\rho}}(M_\rho,M_\pi,m,T)=\frac{N_c}{16\pi^2}\int\limits_{\lambda_{M_\rho}}^{\Lambda}d\mathrm{k}\frac{\mathrm{k}\tanh\left(\frac{E_\mathrm{k}}{2T}\right)}{|\vec{p}|E(M_\rho^2-4E^2)}$$
$$\times\left[\ln\left(\frac{(M_\pi^2+2\mathrm{k}|\vec{p}|)^2-E^2M_\rho^2}{(M_\pi^2-2\mathrm{k}|\vec{p}|)^2-E^2M_\rho^2}\right)\right.$$
$$\left.+\frac{M_\rho}{2E}\ln\left(\frac{M_\pi^4-(EM_\rho-2\mathrm{k}|\vec{p}|)^2}{M_\pi^4-(EM_\rho+2\mathrm{k}|\vec{p}|)^2}\right)\right]. \tag{41}$$

The dependence of the constituent quark mass on the temperature is obtained from the gap equation (5) where integral I_1 is already T-dependent. After we know the temperature dependence of m, I_1, I_2, $\tilde{I}_2$, and I_3, using formulas (13), (14), (18), (19), (24), and (31), we can determine the temperature dependence of F_π, quark and meson masses, coupling constants, and meson decay widths. The results are shown on Figs. 4–7.

The $\sigma\to\pi\pi$ decay width is calculated by the formula:

$$\Gamma_{\sigma\to2\pi}(T)=\frac{3|A_{\sigma\to2\pi}(T)|^2}{32\pi M_\sigma}\sqrt{1-\frac{4M_\pi^2}{M_\sigma^2}}\coth\left(\frac{M_\sigma}{4T}\right), \tag{42}$$

$$A_{\sigma\to2\pi}(T)=\frac{2m(T)Z[1+\delta]\sqrt{I_2^{(\lambda_{M_\sigma},\Lambda)}(M_\sigma,m,T)}}{I_2^{(\lambda_{M_\pi}\ \Lambda)}(M_\pi,m,T)}, \tag{43}$$

where δ is defined in (36). The cotangent in (42) appeared due to the interaction with the pion gas in the final state. Analogously, one has for the ρ-meson:

$$\Gamma_{\rho\to2\pi}(T)=\frac{|A_{\rho\to2\pi}(T)|^2M_\rho}{48\pi}\left(1-\frac{4M_\pi^2}{M_\rho^2}\right)^{\frac{3}{2}}\coth\left(\frac{M_\rho}{4T}\right), \tag{44}$$

$$A_{\rho\to2\pi}(T)=\frac{\sqrt{3I_2^{(\lambda_{M_\rho},\Lambda)}(M_\rho,m,T)}}{\sqrt{2}I_2^{(\lambda_{M_\pi},\Lambda)}(M_\pi,m,T)}$$
$$\times\left(1+\frac{2M_\pi^2J_{3V}^{\lambda_{M_\rho}}(M_\rho,M_\pi,m,T)}{I_2^{(\lambda_{M_\rho}\ \Lambda)}(M_\rho,m,T)}\right). \tag{45}$$

The quantity $J_{3V}^{\lambda_{M_\rho}}(M_\rho,M_\pi,m,T)$ is derived from $J_{3V}^{\lambda_{M_\rho}}(M_\rho,M_\pi,m)$ (see (27)) by replacing all integrals with ones depending on temperature.

The critical temperature T_c is determined by the condition that the pion mass is equal to the sum of the masses of its constituents (the Mott point, see Eq. (23)). From this, one finds $T_c \approx 186$ MeV and $m_c \approx 86$ MeV. Thus the lightest meson (pion) is also allowed to decay into its constituents, quarks, at $T \geq T_c$. For the IR cut-off scheme considered here, other mesons also decay into free quarks if $T \geq T_c$[2].

Finally, we have the following picture. At low T, the σ- and ρ-mesons decay mostly into two pions. The pion is stable since electroweak decay channels can be neglected here compared to the strong ones. At higher T, the ρ-meson still has a noticeable decay width. Unlike the ρ-meson, the width of σ-meson first rises at $T = 100$–150 MeV and then falls down to zero near $T = 170$ MeV. An increasing of the width is due to the interaction with the pion gas in the final state, which leads to an additional factor increasing with temperature. Above T_c, all mesons are allowed to decay into quark-antiquark pairs, and the ρ-meson also decays into pions. It is interesting to note that the σ-meson is stable in the temperature range from 170 MeV to T_c. Here, only its electroweak decays are possible, they are small and can be neglected. Thus we have obtained almost stable scalar meson states freely propagating through hot matter as a precursor of the chiral/ deconfinement transition.

To estimate the decay widths of π-, σ- and ρ-mesons into free quarks, one should evaluate the imaginary part of the corresponding meson propagator that appears if $T > T_c$. One thereby has:

$$\Gamma_{\pi\to\bar{q}q}(T) = \frac{M_\pi \mathrm{Im} I_2^{(\lambda_{M_\pi},\Lambda)}(M_\pi, m, T)}{\mathrm{Re} I_2^{(\lambda_{M_\pi},\Lambda)}(M_\pi, m, T)}, \tag{46}$$

$$\Gamma_{\sigma\to\bar{q}q}(T) = \frac{[M_\sigma^2 - 4m(T)^2]\mathrm{Im} I_2^{(\lambda_{M_\sigma},\Lambda)}(M_\sigma, m, T)}{M_\sigma \mathrm{Re} I_2^{(\lambda_{M_\sigma},\Lambda)}(M_\sigma, m, T)}, \tag{47}$$

$$\Gamma_{\rho\to\bar{q}q}(T) = \frac{M_\rho \mathrm{Im} I_2^{(\lambda_{M_\rho},\Lambda)}(M_\rho, m, T)}{\mathrm{Re} I_2^{(\lambda_{M_\rho},\Lambda)}(M_\rho, m, T)}. \tag{48}$$

The results are shown in Fig. 7 by dashed and dash-dotted lines.

7 Discussion and conclusion

In this paper, we have investigated an extension of the NJL model for the light non-strange meson sector of QCD, where the interaction of u- and d-quarks is represented by four-fermion vertices and the phenomenon of quark confinement is taken into account through the elimination of non-physical quark-antiquark thresholds. This extension of the NJL model describes properties of the π-, σ- and ρ-mesons in satisfactory agreement with experiment and with low-energy theorems. The model parameters are obtained by fitting the model so that it reproduces the experimental values of the pion and ρ-meson masses, the pion decay constant F_π, and the ρ-meson decay constant g_ρ. Moreover, it has been shown that, for the π-, σ- and ρ-mesons, unphysical quark-antiquark thresholds

[2]Note that in the chiral limit ($m^0 = 0$), chiral symmetry is restored at T_c.

do not appear up to the critical temperature if the IR cut-off of the form introduced here is applied.

Let us emphasize that in our model, unlike the standard NJL model [2, 3, 4, 5], we have two cut-offs: the UV cut-off that eliminates the UV divergences and the IR cut-off which provides the confinement of quarks. The UV cut-off determines the dimension of the domain of SBCS where quarks are bosonized. It is chosen to be the same for all sorts of mesons. The second cut-off, λ_M, is introduced into the model in analogy with the bag-model [16, 17, 18] and describes finite dimensions of mesons. We suppose that heavier mesons have smaller radii, therefore the IR cut-off is chosen different for various mesons, being roughly proportional to the meson mass. On the other hand, from the requirement of the absence of quark-antiquark thresholds for $T < T_c$, we determine more certainly the form of the IR cut-off. It is easy to make sure that the IR cut-off of the form (22) satisfies this condition.

The critical temperature is defined as the one at which the pion mass equals the sum of the masses of constituent quarks (the so called Mott point). Thus, after the matter reachs T_c, the pion became unstable as the other mesons and they all are allowed to decay into free quarks under such conditions. This scenario is provided by the IR cut-off scheme implemented in the present work. Although, only scalar, pseudoscalar, and vector mesons have been considered, the axial-vector meson can also be treated the same way, and no unphysical $\bar{q}q$ thresholds will appear for it if $T < T_c$.

Let us note that the introduction of the IR cut-off has not dramatically changed the basic model parameters when compared to a the standard NJL model case [31] with $\lambda_P = 0$. For example, the UV cut-off increased from 1.03 GeV up to 1.09 GeV, the constituent quark mass decreased from 280 MeV down to 242 MeV, the constant G_1 also decreased from 3.48 GeV^{-2} down to 2.98 GeV^{-2}. The current quark mass has almost not changed its value 2.1 MeV. The mass and width of the σ-meson, obtained in this model, are in their experimental bounds [25, 28].

The mechanism of the confinement of quarks that we introduced in our model allows us to take into account the dependence of various quantities on external momenta. As a result, we managed to estimate additional contributions to the amplitudes of $\sigma \to \pi\pi$, $\rho \to \pi\pi$ that are proportional to meson masses squared. It turned out that for the decay $\rho \to \pi\pi$ these corrections were small, and for the decay $\sigma \to \pi\pi$ they made about 30% of the amplitude and decreased the decay rate by half. Taking into account these contributions may be important if one wants to describe such quantities as form factors occurring in various processes, meson radii, scattering lengths, polarizability etc.

The σ- and ρ-mesons, considered here, can play an important rôle as intermediate resonances in the processes occurring in the hot hadron matter created in ultra-relativistic heavy-ion collisions. In particular, a proper consideration of these states can be useful for the explanation and prediction of signals witnessing CSR and the quark deconfinement at the transition of the hadron matter to the quark-gluon plasma phase and vice versa; for example, the low-mass dilepton enhancement observed by the CERES collaboration [34, 35].

All calculations in our model are performed in the Hartree-Fock approximation which does not take into account the next to $1/N_c$ contributions. For applications to the

situation in heavy-ion collisions, where a hot and dense fireball of mesons (predominantly pions) is formed, it is of interest to calculate contributions coming from intermediate pion resonances in the loop diagrams. The properties of the ρ-meson can also be modified due to the cloud of pions in hot matter [36]. An analogous situation is expected for the σ-meson [37]. In our future work we suppose to investigate the next to leading order corrections in the $1/N_c$ expansion.

Acknowledgement

DB thanks Sebastian Schmidt for useful comments and discussions. This work has been supported by RFBR Grant No 00-02-17190 and the Heisenberg-Landau program, 2001. GB, MKV and VLYu acknowledge support by the Ministry for Education and Research of Mecklenburg-Vorpommern and by the DFG Graduiertenkolleg *Strongly correlated many-particle systems*.

References

[1] *Quark-Gluon Plasma 2*, edited by R.C. Hwa (World Scientific, Singapore, 1995).

[2] T. Eguchi, Phys. Rev. D **14**, 2755 (1976); K. Kikkawa, Progr. Theor. Phys. **56**, 947 (1976).

[3] D. Ebert and M.K. Volkov, Yad. Fiz. **36**, 1265 (1982); Z. Phys. C **16**, 205 (1983); M.K. Volkov, Ann. Phys. (N.Y.) **157**, 282 (1984).

[4] M.K. Volkov, Sov. J. Part. Nucl. **17**, 186 (1986).

[5] D. Ebert and H. Reinhardt, Nucl. Phys. B **271**, 188 (1986).

[6] U. Vogl, W. Weise, Progr. Part. Nucl. Phys. **27**, 195 (1991); S.P. Klevansky, Rev. Mod. Phys. **64**, 649 (1992).

[7] G.V. Efimov, M.A. Ivanov, The quark confinement model of hadrons (IOP Publishing Ltd, Bristol, 1993).

[8] F. Gross, J. Milana, Phys. Rev. D **43**, 2401 (1991); D **45**, 969 (1992).

[9] L.S. Celenza, C.M. Shakin, Wei-Dong Sun, J. Szweda and Xiquan Zhu, Phys. Rev. D **51**, 437 (1995); L.S. Celenza, X.-D. Li, C.M. Shakin, Phys. Rev. C **55**, 3083 (1997).

[10] C.D. Roberts and A.G. Williams, Prog. Part. Nucl. Phys. **33**, 477 (1994).

[11] A. Bender, D. Blaschke, Yu.L. Kalinovsky and C.D. Roberts, Phys. Rev. Lett. **77**, 3724 (1996).

[12] D. Ebert, T. Feldmann and H. Reinhardt, Phys. Lett. B **388**, 154 (1996) .

[13] D. Blaschke, G. Burau, M.K. Volkov, V.L. Yudichev, JINR preprint E2-98-227 (1998); Phys. At. Nucl. **62**, 1919 (1999).

[14] G.Burau, D. Blaschke, in: *Understanding Deconfinement in QCD*, World Scientific, Singapore (2000), p. 279.

[15] M.K. Volkov, V.L.Yudichev, Phys. At. Nucl. **63**, 464 (2000).

[16] P.N. Bogoliubov, Ann. Inst. Henri Poincaré **8**, 163 (1967).

[17] A. Chodos, R.L. Jaffe, C.B. Thorn and V. Weisskopf, Phys. Rev. D **9**, 3471 (1974).

[18] A.E. Dorokhov, Yu.A. Zubov, N.I. Kochelev, Part. and Nucl. **23**, 1192 (1992).

[19] S.Chiku and T.Hatsuda, Phys. Rev. D **57**, R6 (1998); *ibid.* D **58**, 076001 (1998).

[20] E.A. Kuraev, M.K. Volkov, D. Blaschke, G. Röpke, S. Schmidt, Phys. Lett. B **424**, 235 (1998); E.A. Kuraev, M.K.Volkov, Phys. At. Nucl. **62**, 128 (1999).

[21] T. Hatsuda and T. Kunihiro, Phys. Rep. **247**, 221 (1994).

[22] *Quark Matter '99*, Proceedings of the XIV International Conference on Ultra-Relativistic Nucleus-Nucleus Collisions, Torino, Italy, Nucl. Phys. A**661** (1999).

[23] D. Blaschke, Yu.L. Kalinovsky, L. Münchov, V.N. Pervushin, G. Röpke, S. Schmidt, Nucl. Phys. A **586**, 711 (1995).

[24] M.K. Volkov and C. Weiss, Phys. Rev. D **56**, 221 (1997).

[25] D.E.Groom *et al.*, Eur. Phys. J. C **15**, 1 (2000).

[26] S. Ishida *et al.*, Progr. Theor. Phys. **95**, 745 (1996); M.Y.Ishida, Progr. Theor. Phys. **101**, 661 (1999); hep-ph/9905259; M.Y. Ishida, T. Komada, S. Ishida, T. Ishida, K. Takamatsu, T. Tsuru, Nucl. Phys. A **675**, 222 (2000).

[27] M. Svec, A. de Lesquen, L. van Rossum, Phys. Rev. D **53**, 2343 (1996); Phys. Rev. **55**, 5727 (1997).

[28] M. Svec, Phys. Rev. D**53**, 2343 (1997).

[29] I.G. Alekseev *et al.* Nucl. Phys. B **541**, 3 (1999).

[30] T. Hatsuda, T. Kunihiro, Phys. Lett. B **145**, 7 (1984); Phys. Rep. **247**, 221 (1994).

[31] D. Ebert, Yu.L. Kalinovsky, L. Münchow, M.K. Volkov, Int. J. Mod. Phys. A **8**, 1295 (1993).

[32] A. Fetter, J. Walecka, Quantum Theory of Many Particle Systems (McGraw Hill, New York, 1971).

[33] J. Kapusta, Finite Temperature Field Theory (Cambridge University Press, Cambridge, 1989).

[34] G. Agakichiev et al., Phys. Rev. Lett. **75**, 1272 (1995); A. Drees *et al.* (CERES Collaboration), Nucl. Phys. A **610**, 536 (1997).

[35] R. Rapp and J. Wambach, Adv. Nucl. Phys. **25**, 1 (2000).

[36] M. Urban, M. Buballa, J. Wambach, Nucl. Phys. A **673**, 357 (2000).

[37] M. Oertel, M. Buballa, J. Wambach, Phys. Atom. Nucl. **64**, 698 (2001).

8 Table captions

1. Model paramters $m_{\rm c}, m, \Lambda, G_1, G_2$ and the mass and width of the σ-meson.

9 Figure captions

1. Three domains for quark propagation in coordinate space and their relation to the UV and IR cut-offs in the momentum space.

2. The quark-loop diagram for the polarization operator of σ and π.

3. The triangle quark diagram describing the decay of ρ- and σ-mesons into two pions.

4. The dynamical quark mass: physical and in the chiral limit ($m^0 = 0$, dash-dotted line), and the pion weak coupling constant F_π, and a half of the pion mass.

5. Masses of σ, π, and ρ. The region above $T_{\rm c}$ is represented by dashed lines.

6. The coupling constants g_π, g_σ, and g_ρ as functions of temperature. The region above $T_{\rm c}$ is represented by dashed lines.

7. The decay widths of π, σ and ρ ($\pi\pi$ and $\bar{q}q$ channels). The region above $T_{\rm c}$ is represented by dashed lines.

10 Tables

Table 1:

$m_{\rm c}$ [MeV]	86
m [MeV]	242
m^0 [MeV]	2.1
Λ [GeV]	1.09
G_1 [GeV]$^{-2}$	2.98
G_2 [GeV]$^{-2}$	11.8
M_σ [MeV]	500
Γ_σ [MeV]	205

11 Figures

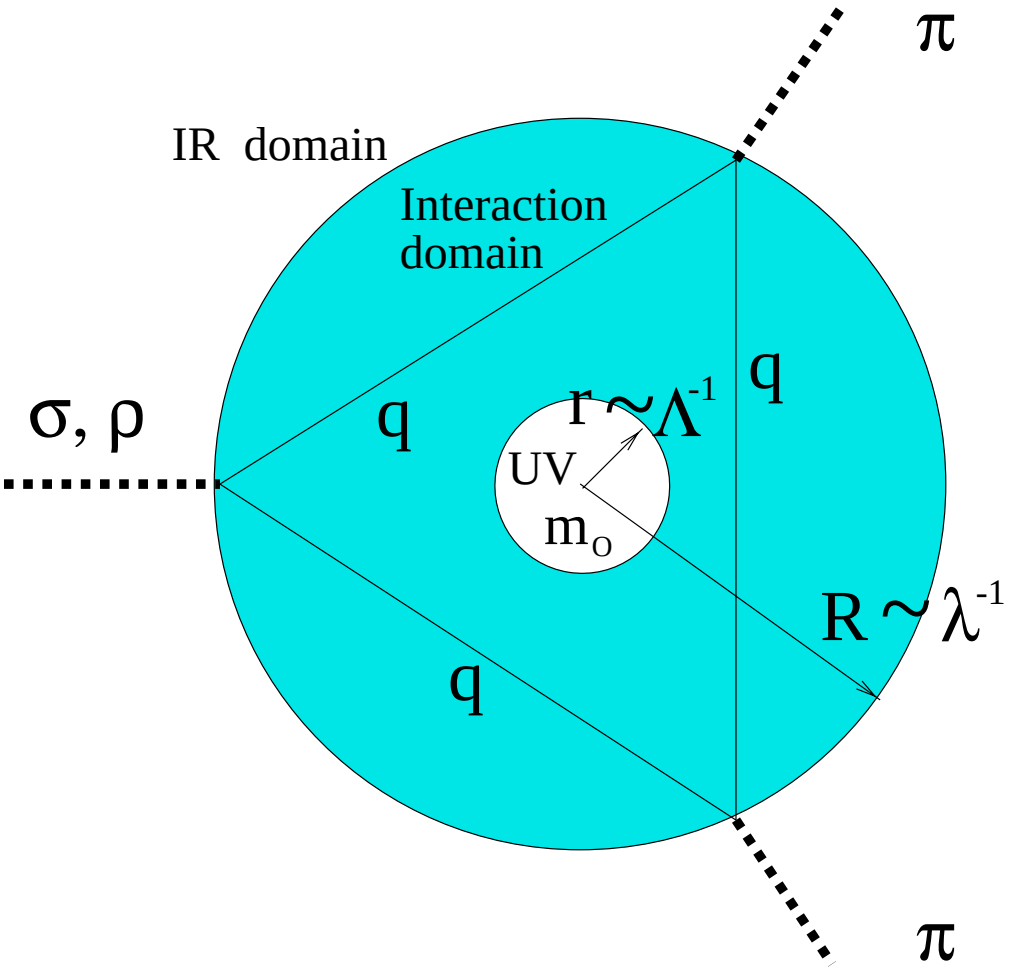

Figure 1:

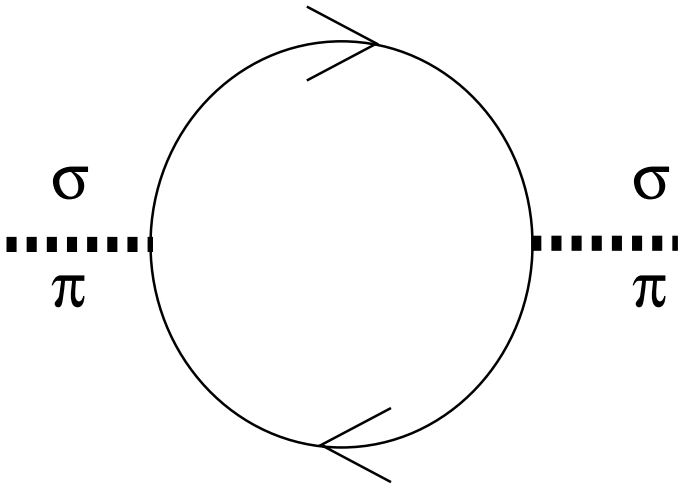

Figure 2:

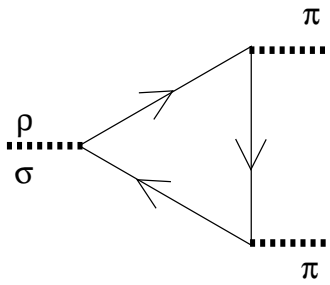

Figure 3:

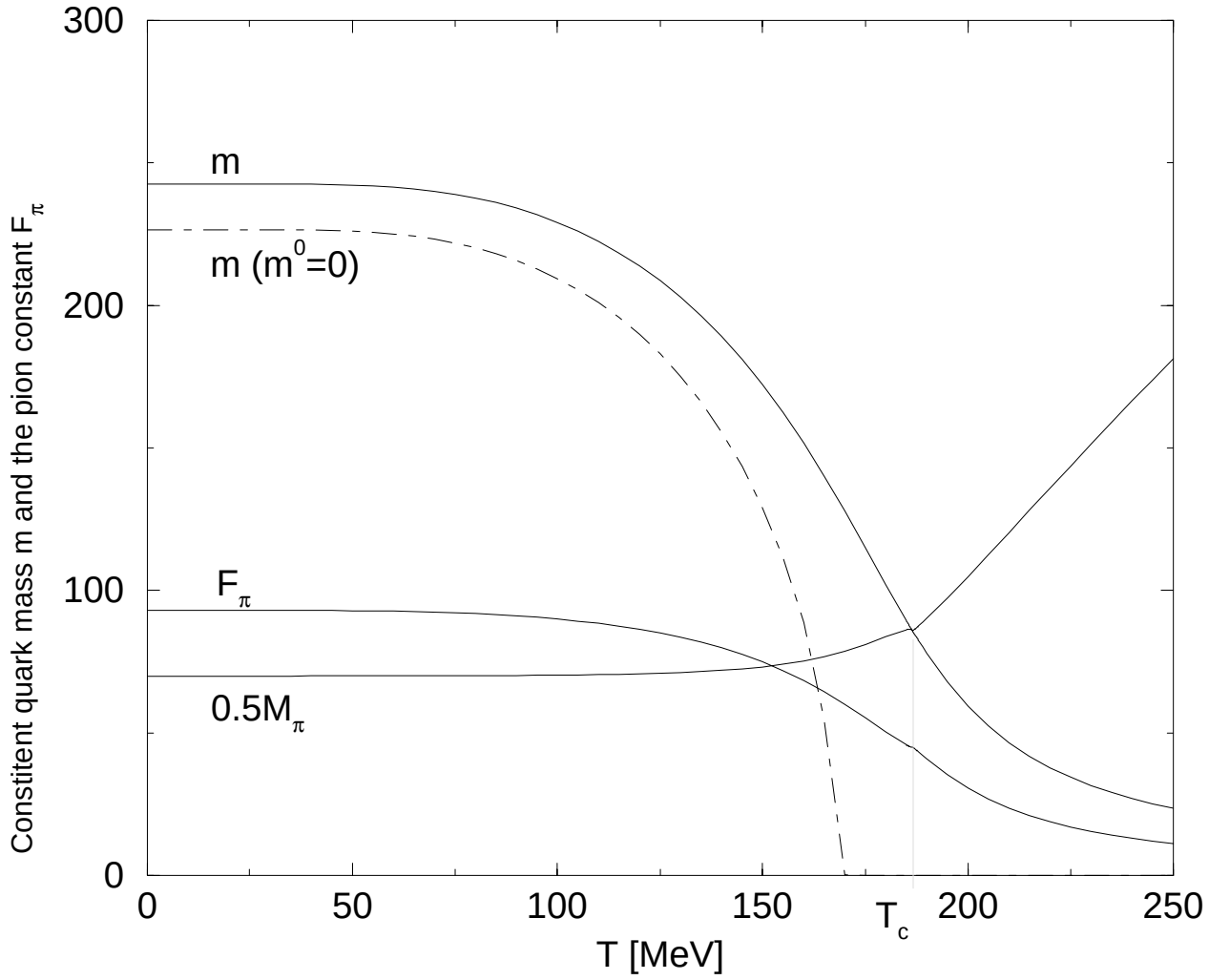
300
200
100
0
m
m (m^0=0)
F_π
$0.5M_\pi$
Constitent quark mass m and the pion constant F_π
0
50
100
150
T_c
200
250
T [MeV]

Figure 4:

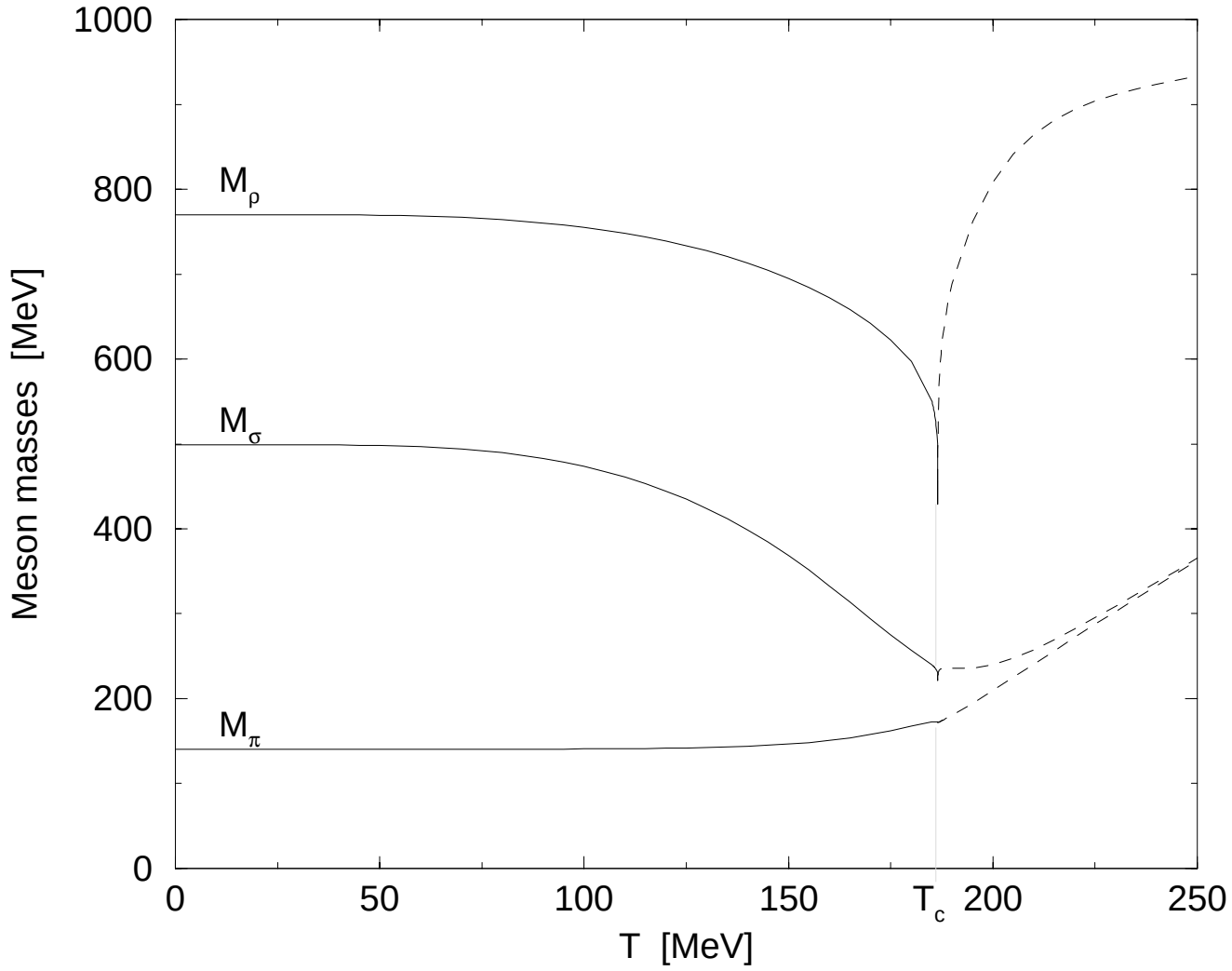
1000
800
600
400
200
0
Meson masses [MeV]
M$_\rho$
M$_\sigma$
M$_\pi$
0
50
100
150
T$_c$
200
250
T [MeV]

Figure 5:

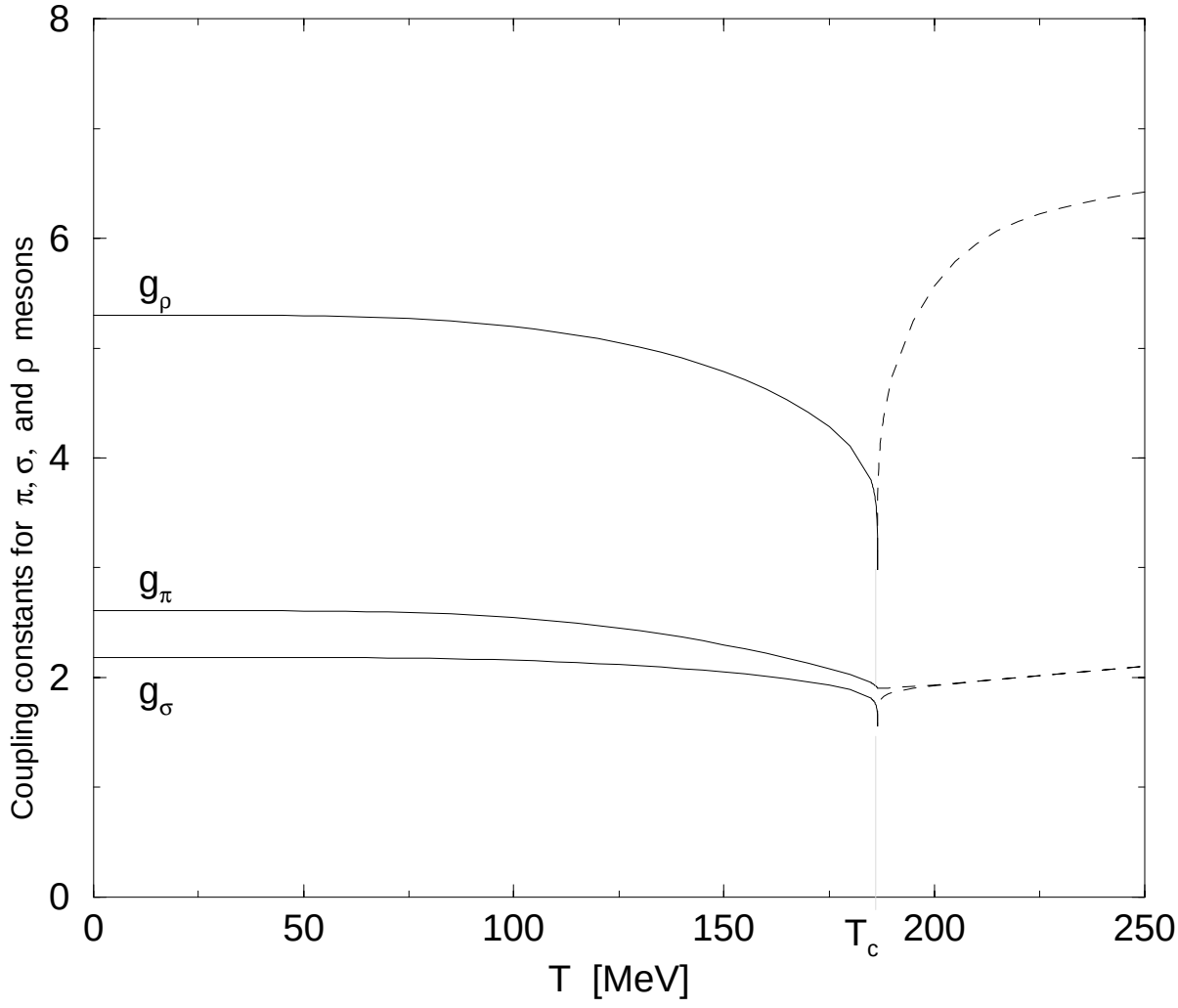
8
6
4
2
0
0
50
100
150
T_c
200
250
T [MeV]
Coupling constants for π, σ, and ρ mesons
g_ρ
g_π
g_σ

Figure 6:

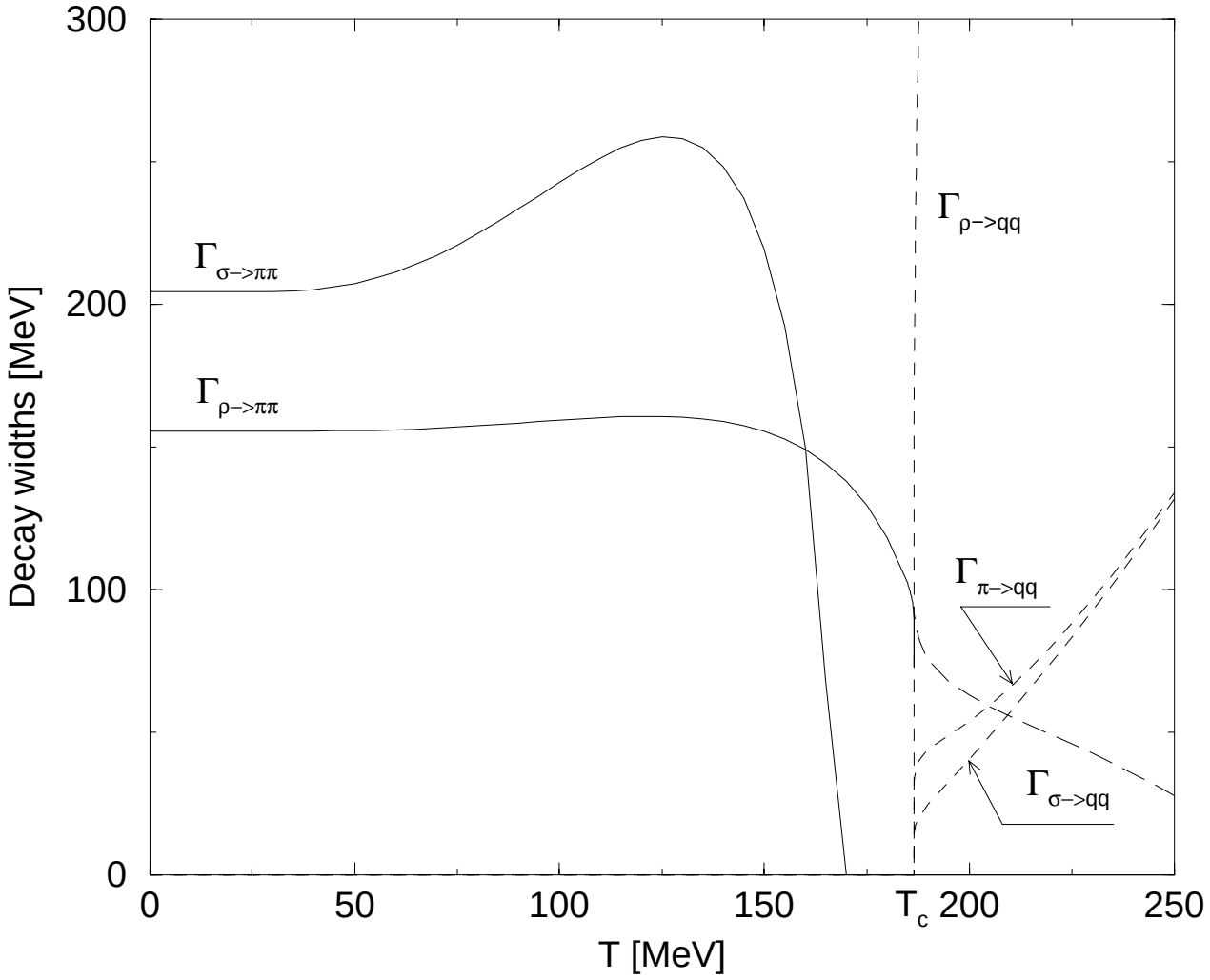
300
200
100
0
Decay widths [MeV]
0
50
100
150
T_c
200
250
T [MeV]
Γ_σ->ππ
Γ_ρ->ππ
Γ_ρ->qq
Γ_π->qq
Γ_σ->qq

Figure 7: